Journal of Solid Mechanics Vol. 9, No. 2 (2017) pp. 434-444

Theoretical, Numerical and Experimental Investigation on Formability of Al3105-St14 Two-Layer Sheet

H. Deilami Azodi *, R. Darabi

Department of Mechanical Engineering, Arak University of Technology, P.O.Box 38135-1177, Arak, Iran

Received 27 March 2017; accepted 23 May 2017

ABSTRACT

Two-layer metallic sheets have wide applications in various industries due to their superlative characteristics. This paper presents analytical model to investigate the formability of two-layer sheets based on Marciniak and Kuckzinsky (M-K) method using Barlat and Lian non-quadratic yield criterion. FEM simulation is also performed to calculate the forming limits based on bifurcation theory. Forming limit diagrams (FLDs) and forming limit stress diagrams (FLSDs) determined by analytical and numerical approaches are compared with experimental results of Al3105-St14 two-layer sheet to verify the validity of theoretical models. The formability of two-layer sheet is also compared with the formability of its components. The results show that the forming limit diagram of two-layer sheet is located between the FLDs of separate layers. The effects of the anisotropy and the orientation of layers on formability of two-layer sheet are studied. The higher formability will be achieved in the case of coincidence of rolling directions of layers.

Keywords : Two-layer metallic sheet; Forming limit diagram (FLD); Forming limit stress diagram (FLSD); M-K theory; Bifurcation theory.

1 INTRODUCTION

IN recent years, two-layer metallic sheets are used increasingly in various industries due to increasing demands for resistance to corrosion and abrasion, creating insulation and weight loss. Formability of metal sheets is limited by localized necking and plastic instability. Forming Limit Diagram (FLD) is a useful tool for evaluation sheet metal formability over various loading paths. The concept of FLD was proposed by Keeler [1] and Goodwin [2]. Various studies have been done on formability of multi-layer sheets.

Semiatin and Piehler studied the deformation of aluminum coated steel sheet and steel coated aluminum sheet. They investigated the formability of sheets based on defuse and localized necking [3,4]. In 1996 Mori and Kurimoto studied the formability of Al1100-SUS340 sheets produced by hot rolling, experimentally. They used stretch forming test with a hemispherical punch and deep drawing process with cylindrical punch to obtain the FLDs. They showed that better formability will be obtained when the aluminum sheet is the outer layer [5]. Yushido and Hino investigated formability of stainless steel-clad aluminum sheets under plane stress condition. They used Hill's localized necking theory for determining the left hand side of the FLD and Marciniak-Kuckzinsky (M-K) method to obtain the right hand side of the FLD [6]. In 2003 Kim et al. derived the FLDs of AA5182/polypropylene/AA5182 sandwich plates produced by rolling process. They applied M-K methods using Hill's quadratic and Barlat yield criteria to determine limit strains in analytical model. They concluded that negative effect of strain hardening

*Corresponding author. Tel.: +98 86 33400662; Fax: +98 86 33670020.
*E-mail address: hdazodi@arakut.ac.ir (*H.Deilami Azodi).

exponent can be disappeared by positive effect of the higher strain rate sensitivity [7]. Lang et al. in 2005 carried out a numerical and experimental investigation on hydroforming of multi-layer sheet with a thin flexible layer in the middle. They showed the better formability occurred when the friction coefficient between layers is high and the formability is controlled by side layers [8]. Jalali et al. studied formability of Al1100-St12 two-layer sheet theoretically and experimentally. They compared the FLD of two-layer sheet with those obtained for its components. They showed that there is good compatibility between theoretical and experimental results and formability of two-layer sheet is better than the component having lower formability [9]. In 2012 jalali et al. investigated the influence of material properties of components on formability of two-layer metallic sheets by theoretical and experimental methods. They illustrated the FLD of two-layer sheet is located between FLDs of its components, depends on material properties of the components [10]. In 2012 Liu et al. studied on forming limit diagram of AA5052/polyethylene/AA5052 sandwich sheets. They used the Gurson–Tvergaard–Needleman (GTN) damage model for numerical investigation and Nakazima test for experimental results. They investigated the interface conditions between skin sheet and core materials using the cohesive zone model. They showed the formability increased by increasing thickness of polyethylene core layer and the formability of sandwich sheet is better than the mono layer model [11]. In 2013, Parsa et al. determined FLD of Al 3105/Polypropylene/Al 3105 sandwich sheets numerically and experimentally. They used the GTN model for numerical investigation [12].

This paper aims to propose an analytical model to investigate the formability of two-layer sheets based on M-K method using Barlat and Lian non-quadratic yield criterion. Bifurcation theory is also used to determine the FLDs numerically. Analytical and numerical results are compared with experimental results of Al3105-St14 two-layer sheet to examine the validity of theoretical approaches.

2 THEORETICAL APPROACH

2.1 Constitutive equations

Non-quadratic yield criterion proposed by Barlat and Lian [13], under the plane stress condition, is expressed in term of principal stress components as:

$$\left|k_1+k_2\right|^M+\left|k_1-k_2\right|^M+\frac{c}{2-c}\left|2k_2\right|^M=\frac{c}{2-c}\bar{\sigma}^M \tag{1}$$

with

$$k_1=\frac{\sigma_1+u\sigma_2}{2}\quad,\quad k_2=\frac{\sigma_1-u\sigma_2}{2}\quad,\quad c=2\sqrt{\frac{r_0}{1+r_0}\frac{r_{90}}{1+r_{90}}}\quad,\quad u=\sqrt{\frac{r_0}{1+r_0}\frac{1+r_{90}}{r_{90}}} \tag{2}$$

where $\bar{\sigma}$ is effective stress and r_0 and r_{90} are anisotropy coefficients. M is related to yield surface shape. The effective stress can be written as:

$$\bar{\sigma}=\left[\frac{2-c}{2}\left(\left|\sigma_1\right|^M+\left|u\sigma_2\right|^M+\frac{c}{2-c}\left|\sigma_1-u\sigma_2\right|^M\right)\right]^{1/M} \tag{3}$$

The exponent M is 6 and 8 for BCC and FCC materials, respectively. The stress ratio, α, the strain ratio, ρ, and the ratio φ are defined as:

$$\alpha=\frac{\sigma_2}{\sigma_1} \tag{4}$$

$$\rho=\frac{\varepsilon_2}{\varepsilon_1} \tag{5}$$

$$\varphi = \frac{\sigma_1}{\bar{\sigma}} \tag{6}$$

Thus, the yield criterion is written as follows:

$$1 + \left|u\alpha\right|^M + \frac{c}{2-c}\left|1-u\alpha\right|^M = \frac{2}{2-c}\varphi^{-M} \tag{7}$$

The associated flow rule is:

$$d\varepsilon_{ij} = d\lambda \frac{\partial f}{\partial \sigma_{ij}} \tag{8}$$

where $d\lambda$ is the plastic multiplier and f is the plastic potential defined by the yield criterion. Using Barlat-Lian yield criterion, the flow rule can be written as:

$$\begin{aligned}
&\frac{d\varepsilon_1}{\mathrm{si}\,gn(\sigma_1)\left|\sigma_1\right|^{M-1} + \mathrm{si}\,gn(\sigma_1 - u\sigma_2)\frac{c}{2-c}\left|\sigma_1 - u\sigma_2\right|^{M-1}} = \\
&\frac{d\varepsilon_2}{\mathrm{si}\,gn(u\sigma_2)u\left|u\sigma_2\right|^{M-1} - \mathrm{si}\,gn(\sigma_1 - u\sigma_2)\frac{uc}{2-c}\left|\sigma_1 - u\sigma_2\right|^{M-1}} = \\
&\frac{-d\varepsilon_3}{\mathrm{si}\,gn(\sigma_1)\left|\sigma_1\right|^{M-1} + \mathrm{si}\,gn(u\sigma_2)u\left|u\sigma_2\right|^{M-1} + \frac{(1-u)c}{2-c}\mathrm{si}\,gn(\sigma_1 - u\sigma_2)\left|\sigma_1 - u\sigma_2\right|^{M-1}\left|\sigma_1 - u\sigma_2\right|^{M-1}} = \frac{d\bar{\varepsilon}}{\frac{2}{2-c}\bar{\sigma}^{M-1}}
\end{aligned} \tag{9}$$

where, $d\varepsilon_1, d\varepsilon_2, d\varepsilon_3$ are the plastic strain incremental components along the principal directions and $d\bar{\varepsilon}$ is the effective strain increment.

2.2 Analytical model based on M-K method using Barlat and Lian non-quadratic yield criterion

M-K theory is one of the earliest theories proposed by Marciniak and Kuczynski [14] to predict the forming limit diagram. Main assumption in this theory is considering a local heterogeneity in the sheet. It is assumed that there is an initial imperfection in the form of a groove related to surface roughness [15] perpendicular to greater principal stress direction. Fig. 1 shows the geometrical model considered in analytical model and the initial groove for a two-layer sheet. The sheet is stretched under biaxial tension by principal stresses σ_1 and σ_2. The rolling directions of layers are coincident and assumed as principle direction. The homogenous and heterogeneous regions are labeled "*a*" and "*b*", respectively.

During the process, thicknesses of each layer in the homogenous and heterogeneous regions change. The thickness of the homogenous region is:

$$t^{a(i)} = t_0^{a(i)}.\exp(\varepsilon_3^{a(i)}) \tag{10}$$

In which $t^{a(i)}$ and $t_0^{a(i)}$ are initial and current thicknesses of layer i in homogenous region, respectively. $\varepsilon_3^{a(i)}$ is thickness strain. The thickness of heterogeneous region is determined as follows [16]:

$$t^{b(i)} = \left(t_0^{a(i)} - 2 * R_Z^{(i)}\right).\exp(\varepsilon_3^{b(i)}) \tag{11}$$

where surface roughness $(R_Z^{(i)})$ is [15]:

$$R_Z^{(i)} = k^{(i)}\sqrt{d_0^{(i)}}.\bar{\varepsilon}^{b(i)} + R_0^{(i)} \tag{12}$$

In which k is the grain size coefficient, d_0 is the grain size, R_0 is the initial roughness and $\bar{\varepsilon}^b$ is the effective strain in heterogeneous region for layer *i*.

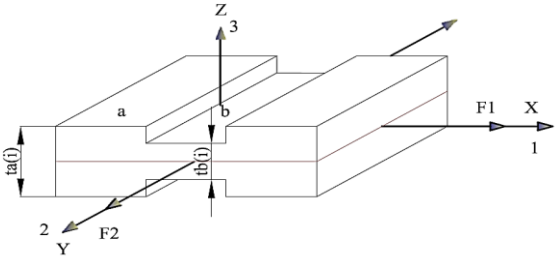

Fig.1
The geometrical model considered in analytical model.

Using the Eq. (9), the strain ratio , ρ , can be written as:

$$\rho^{a(i)or\,b(i)} = \frac{d\varepsilon_2^{a(i)or\,b(i)}}{d\varepsilon_1^{a(i)or\,b(i)}} = \frac{sign(u\sigma_2)u\left|u\sigma_2\right|^{M-1} - sign(\sigma_1+u\sigma_2)\dfrac{cu}{2-c}\left|\sigma_1-u\sigma_2\right|^{M-1}}{sign(\sigma_1)\left|\sigma_1\right|^{M-1} + sign(\sigma_1+u\sigma_2)\dfrac{c}{2-c}\left|\sigma_1-u\sigma_2\right|^{M-1}} \tag{13}$$

Using definition of ρ , incompressibility condition gives:

$$d\varepsilon_3^{a(i)or\,b(i)} = -\left(1+\rho^{a(i)or\,b(i)}\right)d\varepsilon_1^{a(i)or\,b(i)} \tag{14}$$

The compatibility condition is given by:

$$d\varepsilon_2^{b(i)} = d\varepsilon_2^{a(i)} \tag{15}$$

$d\varepsilon_2^{a(i)}$ and $d\varepsilon_2^{b(i)}$ are the strain increments along principal direction 2 in the homogenous and heterogeneous regions for layer *i*, respectively. According to equilibrium condition, the forces acting on homogenous and heterogeneous regions are equal:

$$\sum_{i=1}^{2} F_1^{a(i)} = \sum_{i=1}^{2} F_1^{b(i)} \tag{16}$$

In which $F_1^{a(i)}$ and $F_1^{b(i)}$ are forces applied on direction 1 in regions "*a*" and "*b*" for layer *i* . The Eq. (16) can be written as:

$$\sum_{i=1}^{2} \frac{\sigma_1^{a(i)}}{\bar{\sigma}^{a(i)}}\bar{\sigma}^{a(i)}\mathcal{I}^{a(i)} = \sum_{i=1}^{2} \frac{\sigma_1^{b(i)}}{\bar{\sigma}^{b(i)}}\bar{\sigma}^{b(i)}\mathcal{I}^{b(i)} \tag{17}$$

Assuming isotropic work hardening and strain rate hardening, the behavior of the material for each layer can be expressed as:

$$\bar{\sigma}^{a(i)} = C^{(i)}\left(\bar{\varepsilon}^{(i)}\right)^{n(i)}\left(\dot{\bar{\varepsilon}}^{(i)}\right)^{m(i)} \tag{18}$$

where $C^{(i)}$ is the strength coefficient, $n^{(i)}$ is strain hardening exponent and $m^{(i)}$ is strain sensitivity coefficient for layer *i* .

Using Eq. (9), parameter β is defined as:

$$\beta=\frac{d\bar{\varepsilon}}{d\varepsilon_1}=\frac{\frac{2}{2-c}\bar{\sigma}^{a-1}}{sign(\sigma_1)|\sigma_1|^{a-1}+sign(\sigma_1+u\sigma_2)\frac{c}{2-c}|\sigma_1-u\sigma_2|^{a-1}} \tag{19}$$

Regarding Eqs.(6) and (18), the Eq. (17) can be written as:

$$\sum_{i=1}^{2}\varphi^{a(i)}k^{(i)}\left(\bar{\varepsilon}^{a(i)}+d\bar{\varepsilon}^{a(i)}\right)^{n(i)}t_0^{a(i)}\ \exp\left(\varepsilon_3^{a(i)}\right)=\sum_{i=1}^{2}\varphi^{b(i)}k^{(i)}\left(\bar{\varepsilon}^{b(i)}+d\bar{\varepsilon}^{b(i)}\right)^{n(i)}t_0^{b(i)}\ \exp\left(\varepsilon_3^{b(i)}\right) \tag{20}$$

Based on analytical model presented in this section, the limit strains are determined using following algorithm:

a) At first, by considering a loading path, a finite increment of principal strain $(d\varepsilon_1)$ is imposed on the homogenous regions of two layers. The stress ratio (α), the strain ratio (β), the ratio φ, other principal strain increments $(d\varepsilon_2, d\varepsilon_3)$, effective strain increment $(d\bar{\varepsilon})$ and effective stress $(\bar{\sigma})$ of mentioned region are calculated for each layer.

b) By assuming there is no slip between layers during forming process $(\rho_{layer1}=\rho_{layer2})$, according to equilibrium condition, the stress ratios in heterogeneous regions for two layers $(\alpha^{b(1)},\alpha^{b(2)})$ are determined.

c) In this step, ρ,β and φ in heterogeneous region are determined knowing $(\alpha^{b(1)},\alpha^{b(2)})$ for two layers. The strain increments and the stress components of two layers are obtained in this zone. If the ratio $\frac{d\bar{\varepsilon}^{b(i)}}{d\bar{\varepsilon}^{a(i)}}$ for one of layers becomes greater than 10, the current values of $\varepsilon_2^{a(i)},\varepsilon_1^{a(i)}$ specify a point of the FLD.

d) If the above mentioned ratio is not greater than 10, the calculation route will be repeated by adding a strain increment $d\varepsilon_1$ to the previous amount of strain.

e) The numerical computation will be performed for strain ratios from -0.5 to 1.0.

3 EXPERIMENTAL PROCEDURE

In the experimental study, two-layer sheets consist of 0.5 *mm* thickness aluminum Al3105 sheet and 0.5 *mm* thickness carbon steel St14 sheet were used. The FLDs for 0.5 *mm* thickness Al3105 sheet and 0.5 *mm* thickness St14 sheet were also obtained experimentally. Chemical composition of aluminum alloy and carbon steel sheets are given in Tables 1. and 2. Material properties of used sheets are listed in Table 3. Polyurethane adhesive was used to join two layers.

The experimental FLDs were determined using stretch forming of specimens shown in Fig. 2 by a hemispherical punch. Experimental set up is shown in Fig. 3. The experiments were done with ram speed of 5 *mm/min*. The steel side of specimens was contacted with hemispherical punch. Circular grids of 5 *mm* diameter were printed on surfaces of the specimens to measure the strains experimentally.

The major and minor strains on necking region were calculated from geometry of the deformed grids using

$$\varepsilon_1=\ln\frac{D_1}{D_0} \tag{21}$$

$$\varepsilon_2=\ln\frac{D_2}{D_0} \tag{22}$$

where ε_1 is the major strain and ε_2 is the minor strain. D_0 is initial diameter of grids and D_1 and D_2 are major and minor diameters of deformed grids, respectively.

Fig 4. shows 75 × 200 *mm* specimen after forming.

Forming limit stress diagrams (FLSD) were calculated using determined FLDs as following steps:

a) The strain ratio, ρ, is determined using measured ε_1 and ε_2. Therefore α, β and φ can be derived.

b) Effective strain, $\bar{\varepsilon}$, is calculated using ratio β.

c) $\bar{\sigma}$ is calculated utilizing power law hardening rule.

d) σ_1 is derived using ratio φ.

e) Knowing α and σ_1, another principle stress component, σ_2, can be determined.

Table 1
Chemical composition of aluminum alloy Al3105 sheet.

Ga	V	Cr	Ti	Zn	Fe	Si	Mg	Mn	Cu	Al
0.01	0.01	0.02	0.01	0.33	0.81	0.27	0.61	0.67	0.23	Balance

Table 2
Chemical composition of carbon steel St14 sheet.

C	Si	Mn	P	S	Ti	Co	Al	Sn	Pb
0.07	0.01	0.22	0.01	0.006	0.001	0.004	0.057	0.006	0.001
W	Cr	Ni	Mo	Cu	V	As	Sb	Fe	
0.002	0.001	0.02	0.01	0.01	0.001	0.001	0.001	Balance	

Table 3
Material properties of Al3105 and St14 sheets.

Variables (Unit)	Values	
Material	St14	Al3105
Thickness, *t (mm)*	0.5	0.5
Young's modulus, *E (GPa)*	210	70
Poisson's ratio	0.3	0.33
Density, *(Kg/m^3)*	7850	2700
Strength coefficient, *K (MPa)*	548.44	302
Strain hardening exponent, *n*	0.229	0.103
Strain rate sensitivity exponent, *m*	0.01	0.001
Surface Roughness, $R_0(\mu m)$	4	1.6
Anisotropy parameter, r_0	1.77	0.2
Anisotropy parameter, r_{90}	1.95	0.24
Grain size, $d_0(\mu m)$	10	20

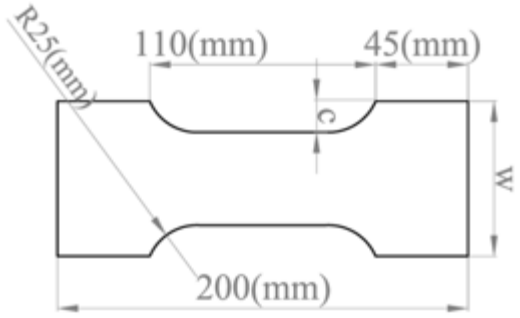

No.	1	2	3	4	5	6	7	8
W(mm)	75	100	125	150	125	150	175	200
C(mm)	17.5	25	25	25	-	-	-	-

Fig.2
The geometries of specimens.

Fig.3
Experimental set-up.

Fig.4
A view of deformed 75 mm×200 mm specimen.

4 NUMERICAL PROCEDURE

In this paper, forming limit diagram for two-layer metallic sheet is determined numerically using finite element code ABAQUS/Explicit. All experimental conditions were duplicated in numerical study. The model was created by ABAQUS/CAE according to geometries shown in Fig. 2. Bifurcation theory was used to determine the FLDs in numerical approach. Punch, die and blank holder were rigid bodies, while two-layer metallic sheets were deformable. Sheets were modeled using four-node shell elements S4R with two integration points. Because of symmetry, only one-quarter of the geometry was modeled. It was assumed that there is no slip between two layers so the tie constraint was used.

An automatic surface to surface contact algorithm was used to define the interfaces between the surfaces of the tooling and the sheet. This algorithm is based on the penalty method.

Coulomb friction model with a constant friction coefficient of 0.1 was used between the sheet-die and sheet-blank holder interface. Higher friction was assumed between the blank and the punch (a friction coefficient of 0.3 was used). Fig. 5 shows simulated 75*mm* × 200*mm* specimen.

Based on bifurcation theory, onset of necking is related to second differentiate of thickness with respect to time and the abrupt changing of thickness strain. Fig. 6 shows the variation of thickness strain of 75*mm*×200*mm* specimen with respect to time.

Fig.7 shows the second differentiate of thickness strain respect to time for the 75*mm* × 200*mm* specimen. The minimum point represents occurrence of necking.

The simulations were performed for 8 specimens given in Fig. 2 to determine the FLD numerically.

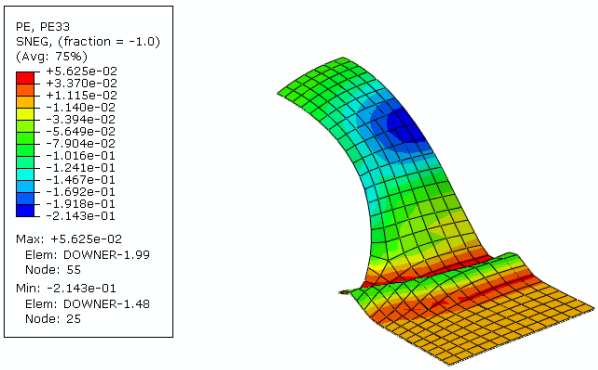

Fig.5
Formed 75 *mm* × 200 *mm* specimen.

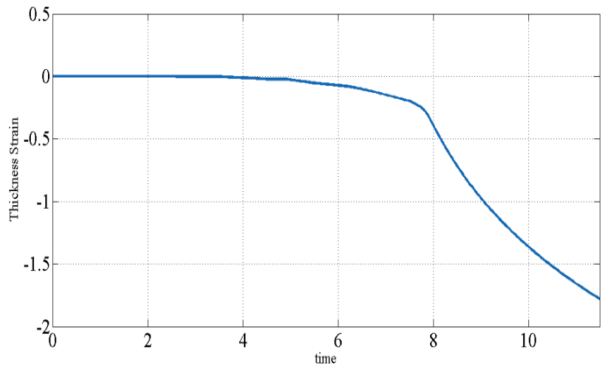

Fig.6
Diagram of thickness strain increment of 75 *mm* × 200 *mm* specimen.

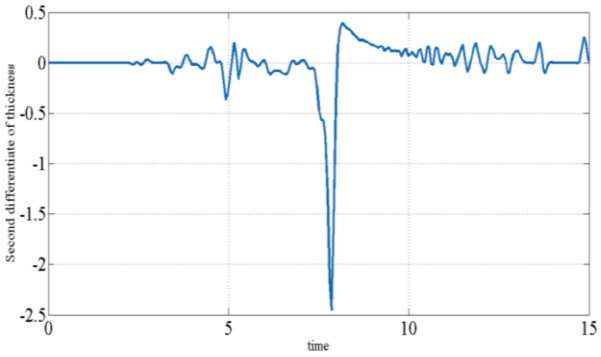

Fig.7
Diagram of second differentiate of thickness strain of 75 *mm* × 200 *mm* specimen.

5 RESULTS AND DISCUSSION

Fig. 8 shows a comparison between forming limit diagrams obtained from analytical, numerical and experimental approaches for Al3105-St14 two-layer sheet. It can be seen that the FLDs calculated from analytical and numerical methods are in a good agreement with experimental results.

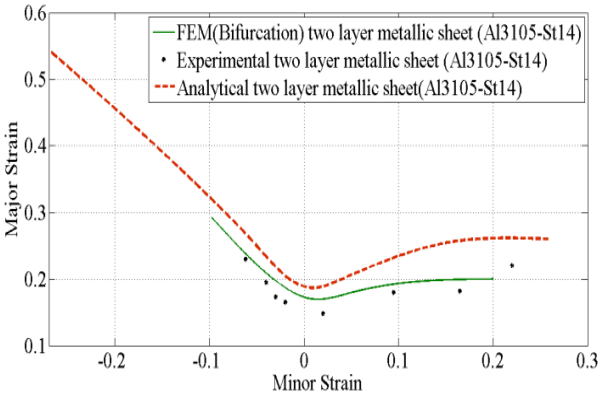

Fig.8
Comparison of analytical, numerical and experimental forming limit diagrams for Al3105-St14 two-layer sheet.

Fig. 9 shows the analytical and experimental FLDs of Al3105-St14 two-layer sheet compared with FLDs of its components. It can be seen that the FLD of two-layer sheet is located between the FLDs of separated layers. The exact location depends on mechanical and geometrical properties of layers. It can be resulted that the formability of two-layer sheet is better than the component with lower formability.

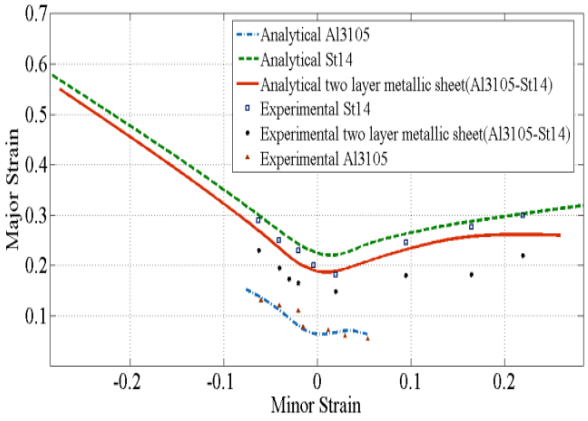

Fig.9
Comparison of analytical and experimental FLDs of Al3105-St14 two-layer sheet with FLDs of separate layers.

Fig.10 represents formability of Al3105-St14 two-layer sheet determined from analytical, numerical and experimental approaches in stress space. The forming limit stress diagram is a more reliable tool for expression of formability rather than the FLD, due to its independence on straining path.

The influence of Barlat-Lian yield surface shape on forming limit diagram of two-layer sheet has been investigated. Fig. 11 shows the forming limit diagram of two-layer sheet using different exponent for yield function. The results demonstrate that *M* affects forming limits on right and left hand sides of the FLD, whereas it has no effect in plane strain region.

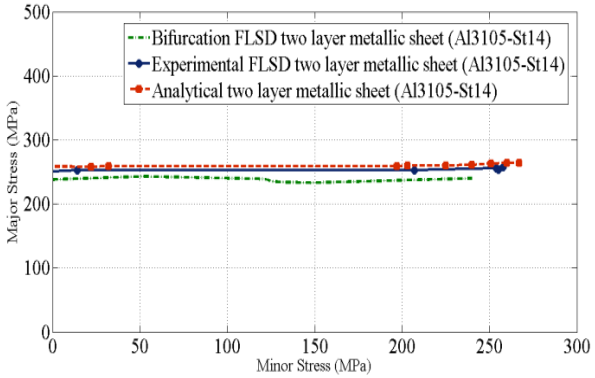

Fig.10
Analytical, numerical and experimental forming limit stress diagrams for Al3105-St14 two-layer sheet.

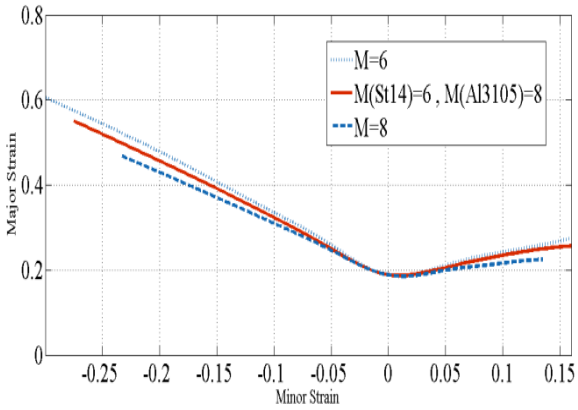

Fig.11
The effect of the exponent of yield function on forming limit diagram of Al3105-St14 two-layer sheet.

The effect of anisotropy of layers on formability of two-layer sheet is shown in Fig. 12. The results indicate that anisotropy of the layer with lower formability is more effective than that of the layer with higher formability, in the left hand side of the FLD. The effect of anisotropy of layers on forming limits of two-layer sheet is not considerable in the right hand side of the FLD.

The effect of orientation of layers on formability of two-layer sheet is represented in Fig. 13. Forming limit diagrams has been determined in the cases of coincidence and perpendicularity of rolling directions of layers. The results show that slightly more formability can be achieved when the rolling directions of two layers are coinciding.

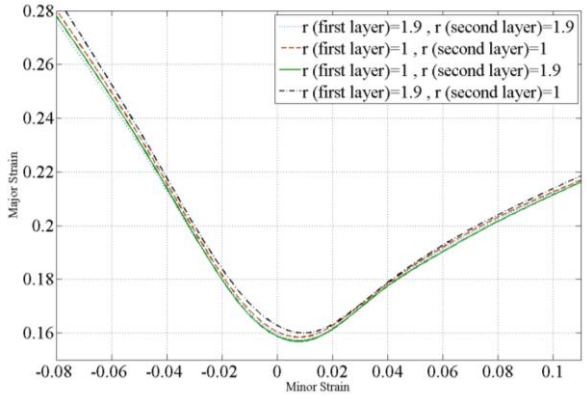

Fig.12
The effect of anisotropy of layers on formability of two-layer sheet.

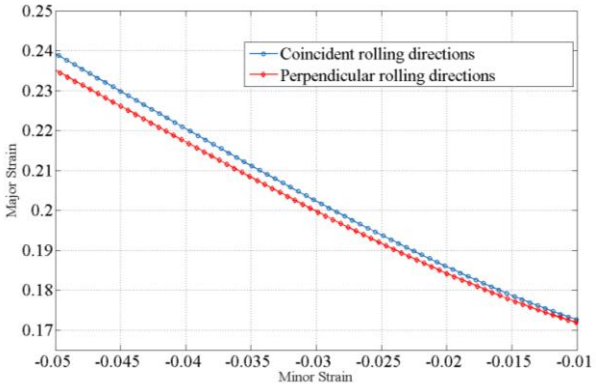

Fig.13
The effect of orientation of layers on forming limit diagram of two-layer sheet.

6 CONCLUSIONS

In this paper, an analytical model was presented to investigate the formability of two-layer sheets based on M-K method using Barlat and Lian non-quadratic yield criterion. FLDs were also calculated based on Bifurcation theory using finite element method. The forming limit stress diagrams were calculated using determined FLDs. Analytical and numerical FLDs and FLSDs were compared with experimental results of Al3105-St14 two-layer sheet, and a good agreement was seen. It can be concluded that:

The forming limit diagram of two-layer sheet is located between FLDs of separate layers.

Formability of two-layer sheet is better than the layer with lower formability.

The exponent of yield function affects forming limits on right and left hand sides of the FLD. It has no effect in plane strain region.

Anisotropy of layers has no significant effect on right hand side of the FLD. In the left hand side, forming limits are mainly affected by anisotropy of layer with lower formability.

The higher formability will be resulted in the case of coincidence of rolling directions of layers.

REFERENCES

[1] Keeler S. P., 1968, Circular grid system - a valuable aid for evaluating sheet metal formability, *SAE International* **77**: 371-379.

[2] Goodwin G. M. , 1968, Application of strain analysis to sheet metal forming problems in press shop, *SAE International* **77** : 380-387.

[3] Semiatin S. L., Piehler H. R., 1979, Deformation of sandwich sheet materials in uniaxial tension, *Metallurgical Transactions A* **10**: 85-96.

[4] Semiatin S. L., Piehler H. R., 1979, Formability of sandwich sheet materials in plane strain compression and rolling, *Metallurgical Transactions A* **10**: 97-107.

[5] Mori T., Kurimoto S., 1996, Press-formability of stainless steel and aluminum clad sheet, *Journal of Materials Processing Technology* **56**: 242-253.

[6] Yoshida F., Hino R.,1997, Forming limit of stainless steel- clad aluminum sheets under plane stress condition, *Journal of Materials Processing Technology* **63**: 66-71.

[7] Kim K. J., Kim D., Choi S. H., Chung K., Shin K. S., Barlat F., Oh K. H., Youn J. R., 2003, Formability of AA5182/polypropylen/AA5182 sandwich sheets, *Journal of Materials Processing Technology* **139** : 1-7.

[8] Lang L., Danckert J., Nielsen K. B., 2005, Multi-layer sheet hydroforming: experimental and numerical investigation into the very thin layer in the middle, *Journal of Materials Processing Technology* **170**: 524-535.

[9] Jalali Aghchai A., Shakeri M., Mollaei Dariani B., 2008, Theoretical and experimental formability study of two-layer metallic sheet Al1100/St12, *Proceedings* of the Institution of *Mechanical Engineers Part B* , *Journal* of *Engineering Manufacture* **222** (9) : 1131-1138.

[10] Jalali Aghchai A., Shakeri M., Mollaei Dariani B., 2012, Influences of material properties of components on formability of two-layer metallic sheets, *International Journal of Advanced Manufacturing Technology* **66**: 809-823.

[11] Liu J., Liu W., Xue W., 2013, Forming limit diagram prediction of AA5052 /polyethylene /AA5052 sandwich sheets, *Materials & Design* **46**: 112-120.

[12] Parsa M. H., Ettehad M., Matin P. H., 2013, Forming limit diagram determination of Al 3105 sheets and Al 3105/polypropylene/Al 3105 sandwich sheets using numerical calculations and experimental investigation, *Journal of Engineering Materials and Technology* **135**: 031003.

[13] Barlat F., Lian K., 1989, Plastic behavior and stretchability of sheet metals. Part I: A yield function for orthotropic sheets under plane stress conditions, *International Journal of Plasticity* **5**: 51-66.

[14] Marciniak Z., Kuczynski K., 1967, Limit strains in the processes of stretch-forming sheet metal, *International Journal of Mechanical Sciences* **9**: 609-620.

[15] Gronstajski J. Z., Zimniak Z., 1992, The effect of changing of heterogeneity with strain on the forming limit diagram, *Journal of Materials Processing Technology* **34**: 457-464.

[16] Dariani B. M., Azodi H. D., 2003, Finding the optimum Hill index in the determination of the forming limit diagram, *Proceedings* of the Institution of *Mechanical Engineers Part B* , *Journal* of *Engineering Manufacture* **217** (12): 1677-1683.